Gli3 is a novel downstream target of miR-200a with an anti-fibrotic role for progression of liver fibrosis *in vivo* and *in vitro*

LI LI, JIANGHUA RAN, LAN LI, GANG CHEN, SHENGNING ZHANG and YINGJIA WANG

Department of Hepatobiliary Surgery, First People's Hospital of Kunming City, Kunming, Yunnan 650034, P.R. China

Received July 23, 2018; Accepted July 9, 2019

DOI: 10.3892/mmr.2020.10997

Abstract. GLI family zinc finger 3 (Gli3), as the upstream transcriptional activator of hedgehog signaling, has previously been demonstrated to participate in the process of liver fibrosis. The present study aimed to investigate the potential functions of microRNA (miR)-200a and Gli3 in the progression of liver fibrosis. The expression levels of miR-200a and Gli3 in cells and tissues were determined by PCR and western blotting; the interaction of Gli3 and miR-200a was evaluated by bioinformatics analysis and dual-luciferase reporter assay. miR-200a was significantly reduced in serum samples from clinical patients, liver tissues of a carbon tetrachloride (CCl_4)-induced rat model and activated LX2 cells. The expression of α-smooth muscle actin (α-SMA) and albumin at the mRNA and protein levels was increased and decreased in LX2 cells, respectively. However, the expression levels of α-SMA and albumin were reversed and Gli3 expression was markedly decreased in LX2 cells when transfected with miR-200a mimics. In addition, the dual-luciferase reporter assay confirmed the target interaction between miR-200a and Gli3. Finally, following the administration of miR-200a mimics to CCl_4-induced rats, it was revealed that the alterations of α-SMA, albumin and Gli3 presented a similar trend to that in LX2 cells with miR-200a mimics transfection. Taken together, these results indicated that downregulation of miR-200a might enhance the formation of liver fibrosis, probably by targeting Gli3, and elevated miR-200a may attenuate the progression of liver fibrosis by suppressing Gli3. These findings suggested that miR-200a may function as a novel anti-fibrotic agent in liver fibrosis via inhibition of the expression of Gli3.

Introduction

Liver fibrosis is a common outcome of virtually all chronic hepatic injuries, such as viral hepatitis, and is frequently induced by hepatitis B and hepatitis C infection, alcoholic or nonalcoholic steatohepatitis, autoimmune and chronic inflammatory conditions, and metabolic disorders (1,2). If left untreated, fibrosis can progress to clinically evident liver cirrhosis and hepatic failure, ultimately leading to mortality. Current treatments for liver fibrosis are mostly limited to removing the underlying injurious stimulus (where possible), eradicating viruses using antiviral drugs in viral hepatitis, enhancing exercise for nonalcoholic steatohepatitis, and liver transplantation (3). However, many patients with liver fibrosis either do not respond to these treatments or are diagnosed at intermediate or advanced disease stages, where satisfactory curative approaches are often not feasible (4). Additionally, although liver transplantation is a highly successful treatment for end stage liver fibrosis, it is not always possible, due to limited organ availability and the presence of contraindicating comorbidities (5). Therefore, there is an urgent need to develop, test and monitor antifibrotic treatments that can prevent, halt, or even reverse liver fibrosis.

MicroRNAs (miRNAs), a class of short (~22 nt) non-coding RNA molecules, can directly regulate gene expression by specifically binding to the 3'-untranslated region (UTR) of target mRNAs to block translation at the initiation or post-initiation steps, inducing mRNA deadenylation and decay (6). It has been demonstrated that several mammalian miRNAs are implicated in various biological processes, including differentiation, proliferation, oxidative stress resistance and tumor suppression (7). miRNAs are known to be dysregulated in several diseases, including liver fibrosis (8). For example, all miRNA (miR)-29 family members (miR-29a, miR-29b, and miR-29c) are downregulated during the *in vitro* activation of isolated rat and mouse hepatic stellate cells [HSCs, the main extracellular matrix (ECM)-producing cells in the fibrotic liver], and in liver biopsies from patients with advanced liver fibrosis; and miR-29 overexpression in HSCs could significantly reduce collagen I and IV synthesis (9-11). miR-122, mainly enriched in hepatic tissue, regulates the activation of HSCs and liver fibrosis by controlling collagen maturation and ECM production (12); ectopic miR-21 stimulates extracellular signal-regulated kinase 1 signaling in HSCs and induces hepatocyte epithelial-mesenchymal transition by targeting sprouty2 or hepatocyte nuclear factor 4α (13). Thus, these findings were expected to uncover the critical mechanism of liver fibrosis and strongly implied that these dysregulated miRNAs serve a role in the development of liver fibrosis, and could also be explored

Correspondence to: Dr Li Li, Department of Hepatobiliary Surgery, First People's Hospital of Kunming City, 504 Qinnian Road, Kunming, Yunnan 650034, P.R. China
E-mail: li_li_hep@163.com

Key words: liver fibrosis, microRNA-200a, GLI family zinc finger 3

as novel disease markers for the diagnosis or monitoring of the progression of liver fibrosis (14).

Recently, increasing evidence has demonstrated that aberrantly expressed miR-200a is considered to be a regulator in some fibrosis diseases. For instance, miR-200a is significantly downregulated in the lungs of rats with experimental lung fibrosis and patients with idiopathic pulmonary fibrosis (15); miR-200a has been identified to be downregulated in transforming growth factor (TGF)-β1-activated pancreatic stellate cells (PSCs) and forced miR-200a expression could attenuate TGF-β1-induced PSC activation and ECM formation by inhibiting the phosphatase and tensin homolog/AKT/mTOR (16). It has also been reported that increasing expression of miR-200a attenuates HSC proliferation while knocking down miR-200a-promoted HSC proliferation (17,18). In addition, the Hh signaling pathway has been found to be an important pathway responsible for the pathogenesis of liver fibrosis. The GLI family zinc finger (Gli) family, including members Gli1, Gli2 and Gli3, can directly activate the Hh signaling pathway (19). Nevertheless, little is known about the roles of miR-200a and the Gli family in the development of liver fibrosis, and the present study aimed to address this.

Materials and methods

Patients. The participants enrolled in the present study were divided into two groups: Group I comprised 10 patients with liver fibrosis from the Digestive System Department of First People's Hospital of Kunming City; and Group II comprised 10 healthy people from the Health Examination Center of First People's Hospital of Kunming City. Participants were recruited between January 2014 and June 2015. The clinical parameters of patients are listed in Tables SI and SII. Patients who had autoimmune hepatitis, drug-induced injury, alcohol abuse or liver carcinoma were excluded. Prior informed consent was obtained from all patients and the study protocol was approved by the Ethics Committee of First People's Hospital of Kunming City. A fasting blood sample (8 ml) was collected from patients with liver fibrosis and healthy donors during his/her first admission to the hospital. The blood samples were kept at room temperature for 1 h and then cellular components were removed by two consecutive centrifugation steps (1,000 x g for 10 min at 4˚C and 1,800 x g for 3 min at 4˚C, respectively). The supernatant serum was recovered and then stored at -80˚C.

Rat models of liver fibrosis and treatment protocol. The animal experiments were approved by the Ethics Committee of First People's Hospital of Kunming City and complied with the National Institutes of Health Guide for the Care and Use of Laboratory Animals (NIH Publications No. 8023, revised 1978) (20). A total of 25 healthy male Sprague-Dawley (SD) rats (5-6 weeks old) with a mean weight of 180±10 g, were obtained from the Guangdong Province Laboratory Animal Center. All the rats were kept in plastic cages with a stainless steel cover (5 rats in each cage), and all of them were provided with free access to food and water (ordinary tap water) in an air-conditioned room (25˚C and 65% humidity) with a 12-h light/dark cycle. All rats were acclimated for 1 week to reduce the stress response caused by environmental changes, and were then used to establish the liver fibrosis model. The SD rats were randomly divided into the control group (healthy rats), Model-0 week group, Model-2 week group, Model-4 week group, Model-8 week group, with 5 rats in each group. Model + Negative control (NC) group were injected with agomir control via the tail vein, and Model + miR-200a group were injected with miR-200a agomir via the tail vein. miR-200a agomir (5'UAACACUGUCUGGUAACGAUGU3' and agomir control (5'UUUGUACUACACAAAAGUACUG3') were obtained from Guangzhou Ribobio Co., Ltd.

The Model-0 week group received nothing as a control. To induce the rat model of liver fibrosis, 50% carbon tetrachloride (CCl_4) in peanut oil solution (0.1 ml/kg, freshly prepared) was subcutaneously injected to the back of the rats twice a week for 2 weeks, 4 weeks and 8 weeks to establish the Model-2 week group, Model-4 week group and Model-8 week group, respectively. Rats in the Model + NC group and Model + miR-200a group were given 1-10 nmol agomir control or miR-200a agomir during the period of CCl_4 treatment every 3 days for 4 weeks.

All rats were sacrificed by CO_2 inhalation to ameliorate animal suffering after the last dose of CCl_4. Blood was collected from the abdominal aorta, and serum was separated and stored at -80˚C. The livers were removed and processed for further histopathological, reverse transcription-quantitative (RT-q)PCR and western blot analysis (WB).

Cell culture and treatments. Normal hepatocytes, including AML12 (mouse hepatocyte cell line) and L02 (human hepatocyte cell line), both from the American Type Culture Collection (ATCC), and the hepatic stellate cell line LX2 (cat no. CBP60648; Shanghai Cobioer Biotech Co., Ltd), were cultivated in Dulbecco's modified Eagle's medium (DMEM; Gibco; Thermo Fisher Scientific, Inc.) containing 10% fetal bovine serum (FBS; Gibco; Thermo Fisher Scientific, Inc.) and 100 μg/ml penicillin and streptomycin, and incubated in a humidified state of 95% air and 5% CO_2 at 37˚C. When the cells grew to 80% confluence in culture flasks, they were detached with a solution of 0.25% trypsin and 0.002% EDTA (Gibco; Thermo Fisher Scientific, Inc.) and seeded into 6-well plates at a density of $5x10^5$ cells/well for subsequent experiments.

THP-1 cells were used to establish the liver cell fibrosis model as previously described by Prestigiacomo *et al* (21). THP-1 cells purchased from ATCC were grown in RPMI-1640 medium (Gibco; Thermo Fisher Scientific, Inc.) with the addition of 10% FBS and antibiotics (100 IU/ml penicillin and 100 mg/ml streptomycin), and kept at 37˚C under 5% CO_2. THP-1 cells were differentiated into macrophages over 48 h with 5-25 ng/ml phorbol-12-myristate-13-acetate (PMA) treatment, according to a previously published method (22). Then, LX2 cells with the characteristics of an activated hepatic stellate cell (HSC) phenotype were pre-cocultured with the treated THP-1 cells and challenged with LPS (1 μg/ml) (21). After 0, 6, 12, 24 and 48 h, the cells were harvested for subsequent analysis.

293T cells obtained from ATCC were cultured in RPMI-1640 medium supplemented with 10% FBS and 1% antibiotics at 37˚C in a humidified air atmosphere containing 5% CO_2, for the dual luciferase assay.

Hydroxyproline assay. Since hydroxyproline is a basic constituent of collagen structure, its content can serve as indicator of collagen synthesis (23). Hydroxyproline analysis was performed to assess the amount of collagen in liver tissues (24). In brief, the samples were hydrolyzed with 6 M HCl at 130˚C for 12 h. Then, 1 ml hydroxyproline developer (β-dimethylaminobenzaldehyde solution) was added to the samples and standards. The optical densities were measured at 558 nm using a spectrophotometer (Bio-Rad Laboratories, Inc.). Finally, the hydroxyproline/mg liver tissue was calculated according to the standard curve constructed with serial concentrations of commercial hydroxyproline.

Histological assessment. Liver tissues were fixed with 10% formalin at 4˚C for 24 h, and 4-μm-thick slices were stained with 0.2% hematoxylin for 10 min and 0.5% eosin for 1 min at room temperature. Subsequently, liver sections were subjected to Masson's trichrome staining (cat. no. SBJ-0288; Nanjing Senbeijia Biological Technology Co., Ltd). To observe the liver fibrosis, the blue pixel content of the images was obtained using an Olympus optical microscope (Olympus Corporation) at x200 magnification. The degree stages of liver fibrosis in the specimen were graded according to the Ishak scoring system (25). The scoring method for the Ishak scoring system is shown in Table I. An Ishak score of ≥2 was regarded as significant liver fibrosis.

Immunohistochemical staining. Immunohistochemistry was used to measure the α-SMA expression in the liver tissues. In brief, the liver tissues were embedded with paraffin, serially sectioned (thickness, 5 μm) and deparaffinized with xylene. Then, gradient ethanol hydration (85% ethanol for 10 min, 95% ethanol for 10 min and 100% ethanol for 10 min) was performed, and the slices were washed with distilled water. Next, heat-induced antigen retrieval (100˚C; 10 min) was conducted followed by blocking of endogenous peroxide using 3% hydrogen peroxide (H_2O_2) in methanol for 15 min at room temperature. The sections were incubated with a primary monoclonal anti-α-SMA antibody (cat. no. ab32575; 1:300; Abcam) overnight at 4˚C. Negative controls were obtained by omitting the primary antibody. After washing with PBS three times for 3 min each time, the sections were incubated with a horseradish peroxidase-conjugated secondary antibody (1:200; cat. no. BA1056; Wuhan Boster Biological Technology, Ltd., China) for 30 min at room temperature. Then, the sections were washed again with PBS three times for 5 min each time, and positive staining was detected using the DAB Envision System (Dako; Agilent Technologies, Inc.). Finally, light microscopy was used for observation, under which α-SMA-positive cells appeared brown-yellow.

Computational target prediction. TargetScan was used to predict putative miRNAs targeted by Gli3 in the present study (http://www.targetscan.org/mamm_31/).

RNA isolation and RT-qPCR detection of miRNA and mRNA. The expression levels of miR-200a, α-SMA, albumin and Gli3 were examined by RT-qPCR. For miRNA analysis, RNA was extracted using the miRNeasy kit (Qiagen GmbH) according to the manufacturer's protocol, and further purified using an RN easy mini kit (Qiagen GmbH) following the instructions of the supplier. Then, total RNA was reverse transcribed (37˚C for 15 min; 85˚C for 10 sec; holding at 4˚C) using the miRCURY LNA Universal RT miRNA PCR, Polyadenylation and cDNA synthesis kit (Exiqon; Qiagen GmbH). cDNA diluted 1:50 was assayed in 10 ml PCR reactions supplemented with SYBR green according to the protocol for the miRCURY LNA Universal RT miRNA PCR with an ABI PRISM 7500 Sequence Detection System (Applied Biosystems; Thermo Fisher Scientific, Inc.) at 95˚C for 10 min, followed by 40 cycles at 95˚C for 10 sec and 60˚C for 1 min.

For mRNA analysis, the cDNA was synthesized using the PrimeScript RT reagent kit (Epicentre; Illumina, Inc.) RT-PCR thermocycling was performed under the following conditions: 37˚C for 15 min, 85˚C for 10 sec, and holding at 4˚C. Then, the cDNA was subsequently amplified by PCR using a SYBR Green mix (Takara Bio, Inc.) on an ABI PRISM 7500 Sequence Detection System. The PCR was conducted as follows: i) Pre-denaturation at 94˚C for 5 min; ii) 40 cycles of denaturation at 94˚C for 40 sec; ii) annealing at 60˚C for 40 sec; iii) extension at 72˚C for 1 min; and iv) overlap extension at 72˚C for 10 min. The quantification cycle (Cq) value for mRNA was normalized against the Cq value for the internal control, β-actin, while U6 small nuclear RNA was used as an internal control for the relative amount of miRNA. The data were analyzed using the comparative Cq method (26), which was defined as $2^{-\Delta\Delta Cq}$ to express the relationship for target gene expression between the experiment and control groups, where $\Delta\Delta Cq=[Cq\ (\text{target gene})-Cq\ (\beta\text{-actin or U6})]_{\text{experiment group}}-[Cq\ (\text{target gene})-Cq\ (\beta\text{-actin or U6})]_{\text{control group}}$. All primers used in this study are listed in Table II and experiments were repeated ≥3 times.

WB. Total proteins from all samples were lysed in modified RIPA lysis buffer (Beyotime Institute of Biotechnology) with freshly added protease inhibitor cocktail (Beyotime Institute of Biotechnology) at 4˚C for 30 min. Protein concentration was quantified using a BCA protein assay kit (Thermo Fisher Scientific, Inc.). Then, 30 μg of total cellular extracts were separated by 10% SDS-PAGE and immobilized onto a polyvinylidene fluoride membrane (EMD Millipore). Following blocking by 5% skimmed milk at room temperature for 1 h, the membrane was probed with primary antibodies against GAPDH (cat. no. ABCA0467269; 1:1,000; Abmart), α-SMA (1:1,000; Abcam), albumin (1:1,500; Abcam) and Gli3 (cat. no. ab6050; 1:2,000; Abcam) overnight at 4˚C. Subsequently, the membrane was incubated with horseradish peroxidase-conjugated goat-anti-mouse IgG (cat. no. ABCA2267961; 1:12,000; Abmart) or goat-anti-rabbit IgG (cat. no. ABCA2267958; 1:12,000; Abmart) for 1 h at room temperature. Following incubation, the membranes were extensively washed with Tris-buffered saline with 0.1% Tween-20 (TBST) five times for 5 min each time. Immunoreactive bands were visualized using ECL detection reagent (Beyotime Institute of Biotechnology) using Gel imager (Bio-Rad Laboratories, Inc.). Densities of target protein bands were determined with Quantity One version 4.6 (Bio-Rad Laboratories, Inc.). The internal control GAPDH was used to normalize loading variations.

Construction of luciferase plasmids and reporter assay. The 3' UTR of Gli3 fragment containing putative binding

Table I. Sequences of primers used for reverse transcription-quantitative PCR.

miRNA or gene	Primer sequences
miR-200a	RT primer: 5'-CTCAACTGGTGTCGTGGAGTCGGCAATTCAGTTGAGCCAAGTTC-3'
	Forward primer: 5'- ACACTCCAGCTGGGTAACACTGTCTGGTAACG-3'
	Reverse primer: 5'- CTCAACTGGTGTCGTGGA-3'
U6	RT primer: 5'-CTCAACTGGTGTCGTGGAGTCGGCAATTCAGTTGAGAAAAATATGG-3'
	Forward primer: 5'-CTCGCTTCGGCAGCACA-3'
	Reverse primer: 5'-AACGCTTCACGAATTTGCGT-3'
α-SMA (Human)	Forward primer: 5'-GTTCCAGCCATCCTTCATCGG-3'
	Reverse primer: 5'-CCTTCTGCATTCGGTCGGCAA-3'
Albumin (Human)	Forward primer: 5'-CAGAATGCGCTATTAGTTCG-3'
	Reverse primer: 5'-CTGGCGTTTTCTCATGCAA-3'
Gli3 (Human)	Forward primer: 5'- TTTTCCCCTTTAATCTTGCCAT-3'
	Reverse primer: 5'-CCAGTGGCAAATCAACCTCC-3'
β-actin (Human)	Forward primer: 5'-CTCCATCCTGGCCTCGCTGT-3'
	Reverse primer: 5'-GCTGTCACCTTCACCGTTCC-3'
α-SMA (Rat)	Forward primer: 5'-GCGTGACTCACAACGTGCCTA-3'
	Reverse primer: 5'-CCCATCAGGCAGTTCGTAGCTCT-3'
Albumin (Rat)	Forward primer: 5'-GATCTGCCCTCAATAGCTG-3'
	Reverse primer: 5'-TGGCTTCATATTTCTTAGCAA-3'
Gli3 (Rat)	Forward primer: 5'-CTCGACCATTTCCACGGCAAC-3'
	Reverse primer: 5'-TCAGCACAGTGAAGTCTACACC -3'
β-actin (Rat)	Forward primer: 5'- TCAGGTCATCACTATCGGCAAT-3'
	Reverse primer: 5'-AAAGAAAGGGTGTAAAACGCA-3'

miR, microRNA; α-SMA, α-smooth muscle actin; Gli3, GLI-Kruppel 3; WB, western blot analysis; UTR, untranslated region.

sites for miRNA-200a was amplified by PCR from human genomic DNA and cloned into the psiCHECK-2 reporter vector (Promega Corporation). The PCR was conducted as follows: i) Pre-denaturation at 94˚C for 5 min; ii) 40 cycles of denaturation at 94˚C for 40 sec, annealing at 58˚C for 30 sec, extension at 72˚C for 30 sec; and iii) overlap extension at 72˚C for 10 min. The predicted target site was mutated by site-directed mutagenesis (27). For the luciferase reporter assays, the wild-type (WT) or mutated luciferase plasmids and miRNAs, including miRNA-200a mimics, miRNA-200a inhibitor, negative control (NC) plasmid or NC inhibitor, were co-transfected into 293T cells (~80% confluence) using Lipofectamine™ 2000 transfection reagent (cat. no. 11668019; Invitrogen; Thermo Fisher Scientific, Inc.) and each experiment was repeated in triplicate. All of the plasmids contained a GFP reporter, and the transfection efficacy was calculated as the ratio of GFP^+ cells/total cells. The transfection efficiency for miR-200a mimics and inhibitor was detected using laser scanning confocal microscopy at x100 magnification (Fig. S1). Cells were lysed at 48 h post-transfection and luciferase activity was assayed using a dual-luciferase reporter assay system (Promega Corporation). Firefly luciferase activity was normalized to *Renilla* luciferase activity, with ratios of firefly luciferase values/*Renilla*.

Statistical analysis. The statistical analysis was performed using SPSS Statistics Version 18 (SPSS, Inc.) and graphs were generated with GraphPad Prism 5 (GraphPad Software, Inc.). Data are presented as the mean ± standard deviation and comparisons between two groups were made by Tukey's HSD post-hoc test following one-way ANOVA. $P<0.05$ was considered to indicate a statistically significant difference. The correlation between Gli3 and miR-200a was evaluated by linear fit; if the correlation coefficient, R^2, was >0.6, it was considered to indicate a significant correlation.

Results

miR-200a expression levels in serum specimens of liver fibrosis patients and cellular samples. The miR-200a levels in serum specimens and cellular samples were determined using RT-qPCR. As shown in Fig. 1A, a decreased level of miR-200a was observed in serum specimens from patients with liver fibrosis compared with the control group. Meanwhile, the expression of miR-200a in the hepatic stellate cell line LX2 was significantly lower compared with normal AML12 and L02 hepatocytes ($P<0.05$; Fig. 1B). Therefore, the results suggested that miR-200a might be implicated in the process of liver fibrosis.

Animal model observations. Administration of CCl_4 can cause iterative toxic damage in the liver, so it is commonly used to construct models of experimental fibrosis (28). First, hydroxyproline, a surrogate marker for collagen content (29), was detected, and the results showed that hydroxyproline content was gradually increased in the rat model groups over

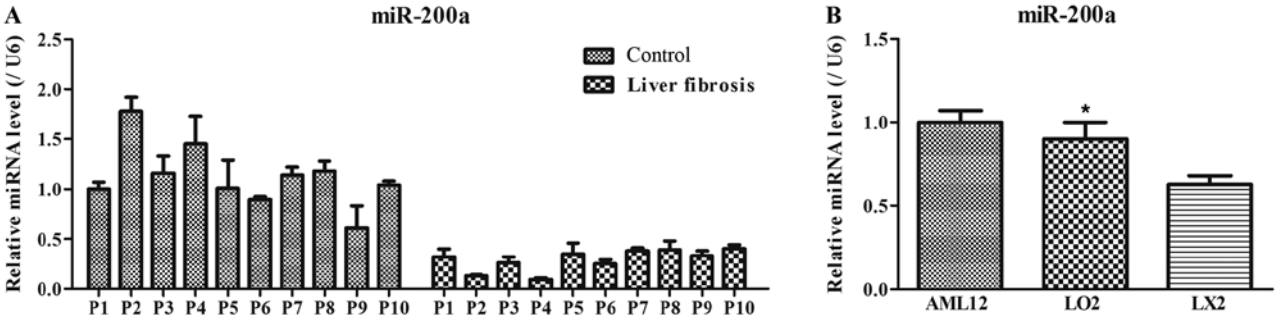

Figure 1. miR-200a levels detected by reverse transcription-quantitative PCR. (A) The levels of miR-200a in blood specimens of patients with liver fibrosis and healthy donors. (B) The expression of miR-200a in the hepatic cell lines AML12, LO2 and LX2. *P<0.05 vs. LX2 group. Fold changes were analyzed using the formula $2^{-\Delta\Delta Cq}$. miRNA/miR, microRNAs; P, participant.

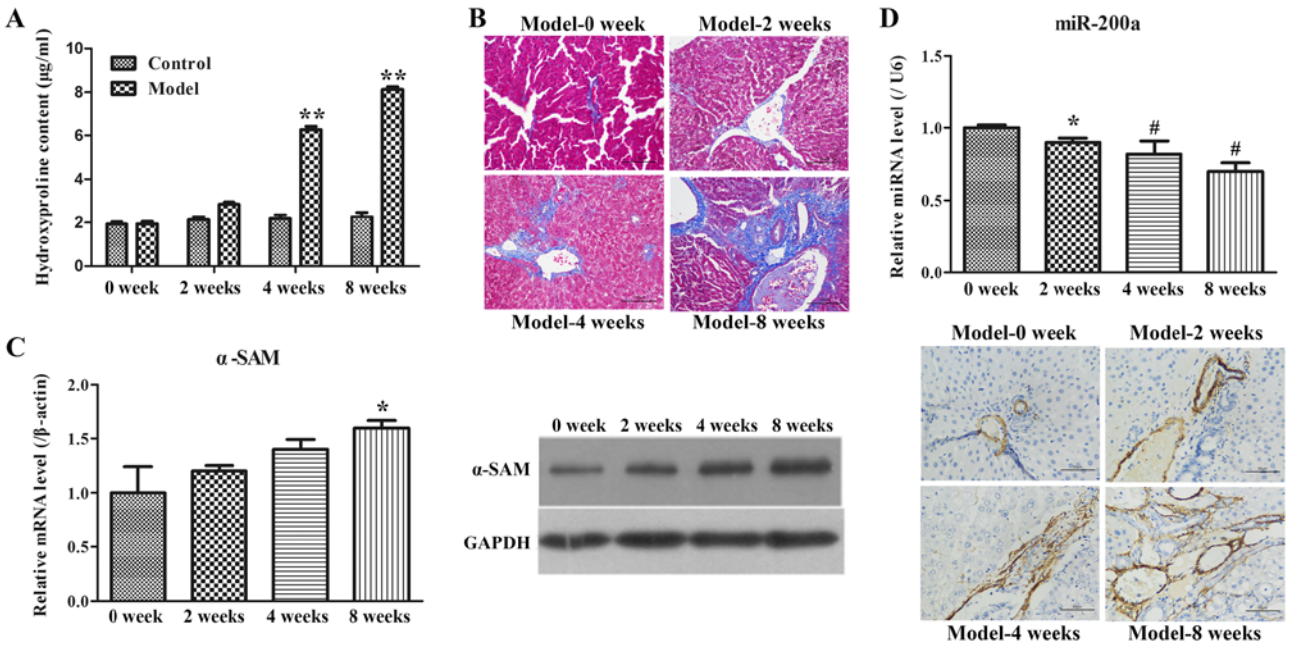

Figure 2. A rat model of liver fibrosis was constructed by administrating CCl_4. (A) Quantification of hydroxyproline content during the course of construction of the liver fibrosis model at different time points. **P<0.01 vs. control group. (B) Histology with hematoxylin and eosin and Masson's staining of liver sections (magnification, x200). (C) The miR-200a levels in liver tissues were examined using RT-qPCR. *P<0.05 vs. 0-week group. #P<0.05 vs. 2 weeks group. (D) α-SMA expression was tested by RT-qPCR, WB and immunohistochemistry methods. *P<0.05 vs. 4-week group. Representative images of WB and imunohistochemistry are given. Data were quantified by comparing to the level of U6. Data are presented as mean ± standard deviation. Scale bar, 50 μm. α-SMA, α-smooth muscle actin; RT-qPCR, reverse transcription-quantitative PCR; WB, western blot analysis; miR/miRNA, microRNA.

time (Fig. 2A). Subsequently, the morphological changes of liver injury and fibrosis were visualized in sections by H&E and Masson's staining. The ISHAK scoring system was used to evaluate the degree of liver fibrosis in the H&E sections (Table II). It was found that rats in Model-0 week group exhibited an ISHAK score of 1 with intact liver tissue structures and very little collagen deposition (Fig. 2B). However, rats in Model-2, Model-4 and Model-8 exhibited an ISHAK score of 2.39, 3.62 and 4.76, respectively, and showed an increased amount of blue collagen deposited in the portal area and interlobular septa of the liver (Table III). Similarly, the Masson-positive area increased with the modeling time and was augmented from 15.17% in Model 0 week to 41.26% in Model 8 week (Table III). Using correlation analysis, it was noted that ISKAK score and Masson-positive area in Table III were negatively correlated with miR-200a expression in Fig. 2C (R^2=0.947 and 0.945 respectively). In order to further evaluate the rat model of liver fibrosis, α-SMA mRNA and protein expression levels were tested by RT-qPCR, WB and immunohistochemistry analysis. As demonstrated in Fig. 2D, an increasing trend of α-SMA mRNA expression was observed over the model progression period. WB also demonstrated similar results. In addition, liver tissues with positive α-SMA expression exhibited yellow or brown granules in immunohistochemical staining. The representative IHC images of each group in Fig. 2D revealed that fewer α-SMA-positive tissues were detected around the blood vessels of liver tissues in the Model-0 week group, whereas the expression of α-SMA was found not only at the vascular walls, but also widely spread at the portal area, fibrous septum and the adjacent hepatic sinusoids in other three groups. These results indicated that the rat model of liver fibrosis was successfully established.

Table II. Description of the ISHAK scoring.

Score	Description
0	No fibrosis
1	Fibrotic expansion of some portal areas, with short fibrous septa
2	Fibrotic expansion of most portal areas, with short fibrous septa
3	Fibrotic expansion of most portal areas, with occasional portal to portal bridging
4	Fibrotic expansion of most portal areas, with marked portal to portal bridging and portal areas to central bridging
5	Marked bridging with occasional nodules
6	Probable to define cirrhosis

Table III. ISHAK score and Masson-positive area of the rat livers.

Assay	Control	Model 0 week	Model 2 week	Model 4 week	Model 8 week
Ishak score	0.00±0.00	1.00±0.13	2.39±0.49	3.62±0.75	4.76±1.01
Masson (%)	2.03±0.28	15.17±2.85	19.37±2.63	25.06±3.55	41.26±4.76

Examination of miR-200a expression in rat model of fibrosis. Based on the lower miR-200a expression in clinical samples, the expression level of miR-200a in the rat model of fibrosis with was further measured using RT-qPCR. It was identified that miR-200a expression was gradually decreased over the model progression period (Fig. 2C). Hence, it was suggested that the decrease in miR-200a expression may be involved in the progression of liver fibrosis.

miR-200a and fibrosis-related gene expression in the co-culture system of LX2 and THP-1 cells. HSCs, such as LX2 cells, serve an important function in the process of liver fibrosis (30), thus LX2 cells were adopted as a cellular model of human hepatic fibrosis. The miR-200a expression was determined by RT-qPCR and it was established that the levels of miR-200a gradually declined in time-dependent manner (Fig. 3A).

α-SMA, as the marker of activated HSCs (30), was evaluated at the mRNA and protein level using RT-qPCR and WB, respectively. The results revealed that upregulated expression of α-SMA was found (Fig. 3B and D). Additionally, changes in albumin were also measured as they are the major predictor of liver fibrosis in patients. Downregulated expression of albumin was observed (Fig. 3C and D). These data further suggested that the co-culture system with activated LX2 cells and miR-200a may serve an important role in the development of liver fibrosis.

Roles of miR-200a in serum specimens. Gli3 is related to liver fibrosis. Thereafter, the expression of Gli3 in the serum was measured. Results demonstrated that the Gli3 level was clearly elevated in liver fibrosis patients compared with the controls (Fig. 4A). Moreover, the Gli3 expression and miR200a expression were negatively correlated, with the R^2 value being 0.69 in the healthy control and 0.73 in the fibrosis patients (Figs. 4B and C and S1).

Roles of miR-200a in activated LX2 cells. In order to further explore the effects of miR-200a during the formation of liver fibrosis, fibrosis-related gene and protein expression (α-SMA, albumin and Gli3) were determined by RT-qPCR and WB in LX2 cells with NC plasmid and miR-200a mimic transfection. It was demonstrated that the mRNA and protein expressions of α-SMA and Gli3 in miR-200a group were notably lower compared with the NC group (Fig. 5A, C and D), whereas the mRNA and protein expression levels of albumin in the miR-200a group were markedly higher than those in the NC group (Fig. 5B and D). Thus, these data demonstrated that miR-200a might suppress α-SMA and Gli3 expression and facilitate albumin expression.

miR-200a directly acts on the 3'-UTRs of Gli3. Through computational target prediction, it was found that the 3'-UTRs of Gli3 contained putative binding sites for miR-200 (Fig. 5E). To verify whether miR-200a directly binds to the 3'-UTRs of Gli3 and causes translational inhibition, dual-luciferase reporter assays were performed using 293T cells. The miR-200a mimics significantly decreased the luciferase activity of the Gli3 3'-UTR-dependent reporter, but it did not affect the luciferase activity of the mutant reporter (Fig. 5E). The mimics control had no effect on either WT or mutant reporter luciferase activity, suggesting that miR-200a might directly act on the 3'-UTRs of Gli3 mRNA.

Effects of over-expression of miR-200a in a rat model of liver fibrosis. Next, miR-200a agomir was used to confirm the role of miR-200a *in vivo*. As demonstrated in Fig. 6, in line with the results of miR-200a mimic-transfected LX2 cells, the mRNA and protein expressions of α-SMA and Gli3 were significantly decreased in the livers of rats receiving miR-200a agomir, while the mRNA and protein expression levels of albumin were significantly increased. Taken together, these data indicated that miR-200a could decrease α-SMA and Gli3 expression, while increasing albumin expression *in vivo* and *in vitro*.

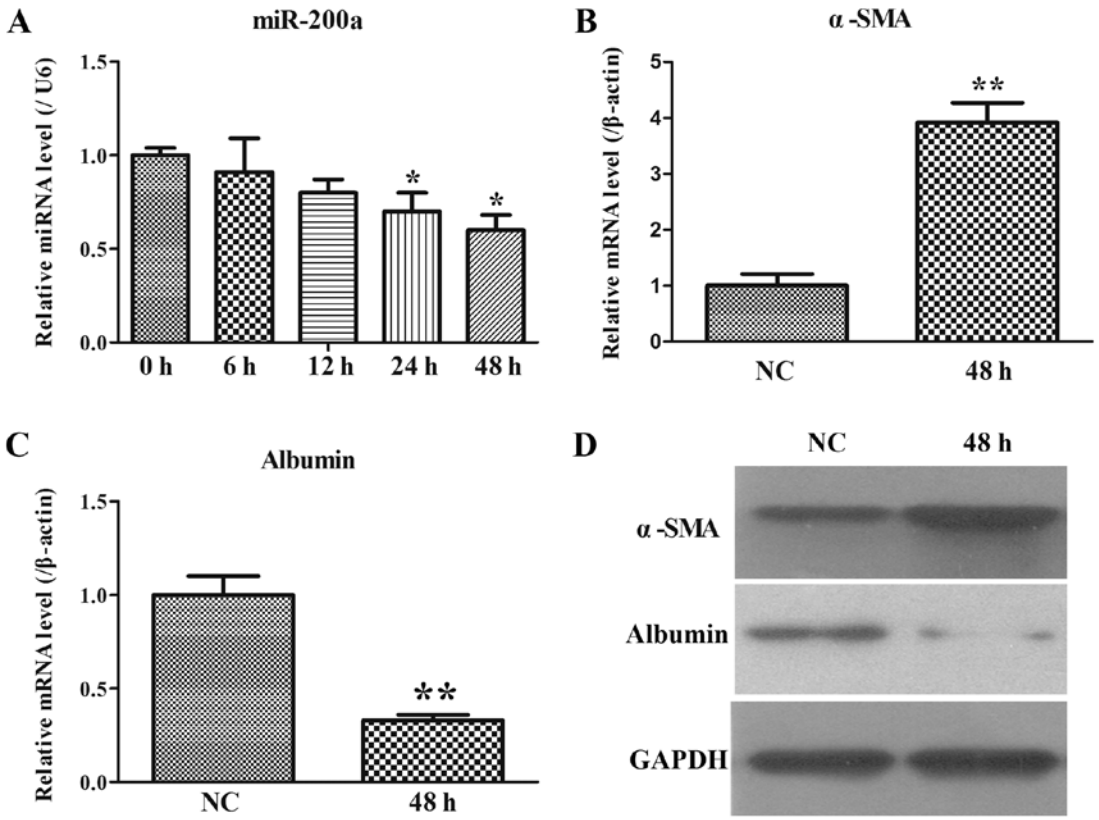

Figure 3. Activation of LX2 cells induced by co-culture with THP-1 cells. (A) miR-200a expression in LX2 cells was examined by RT-qPCR. *P<0.05 vs. 0 h group. (B) The mRNA levels of α-SMA were measured by RT-qPCR. Each value represents the mean ± standard deviation of three experiments. **P<0.01 vs. NC group. (C) The mRNA levels of albumin were assessed by RT-qPCR. Each value represents the mean ± standard deviation of three experiments. **P<0.01 vs. NC group. (D) The protein levels of α-SMA and albumin were analyzed by western blotting and compared to GAPDH. Data are presented as mean ± standard deviation. miR, microRNA; RT-qPCR, reverse transcription-quantitative PCR; α-SMA, α-smooth muscle actin; NC, negative control.

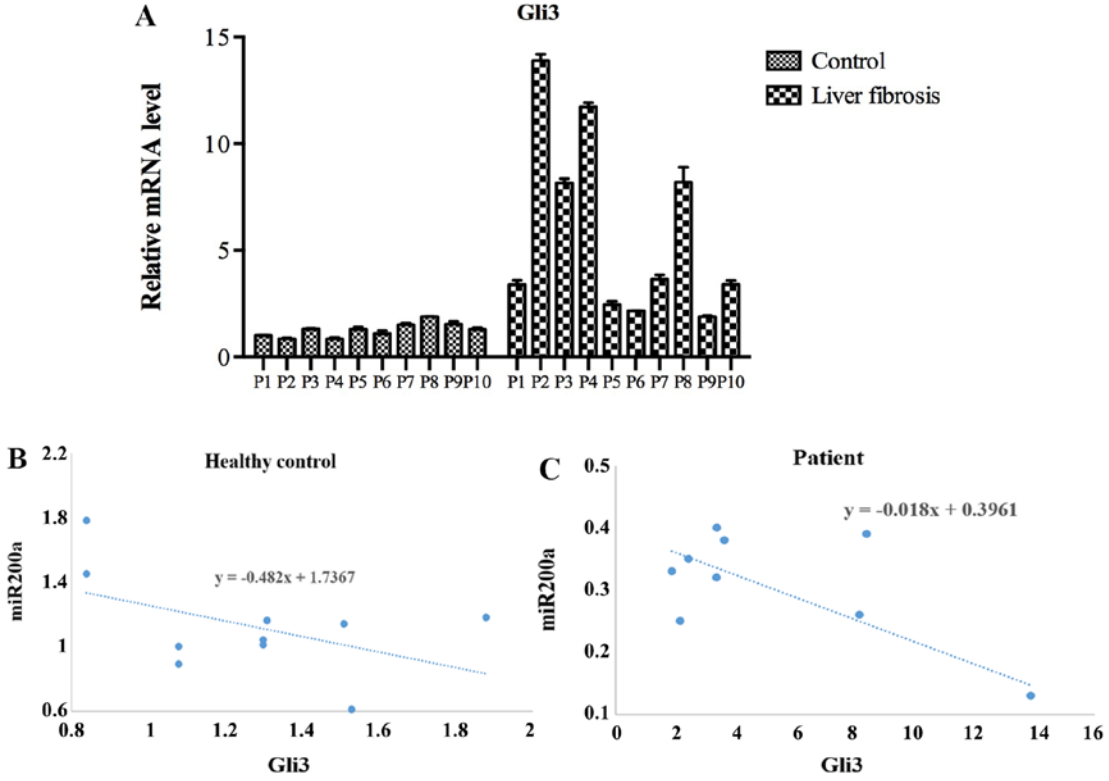

Figure 4. Expression of Gli3 in patients and healthy individuals. (A) Expression of Gli3 mRNA in patients with liver fibrosis and healthy donors. (B) Linear analysis of miR-200a and Gli3 expression in a healthy individual. (C) Linear analysis of miR-200a and Gli3 expression in patients with liver fibrosis. miR, microRNA; Gli3, GLI-Kruppel 3; P, participant.

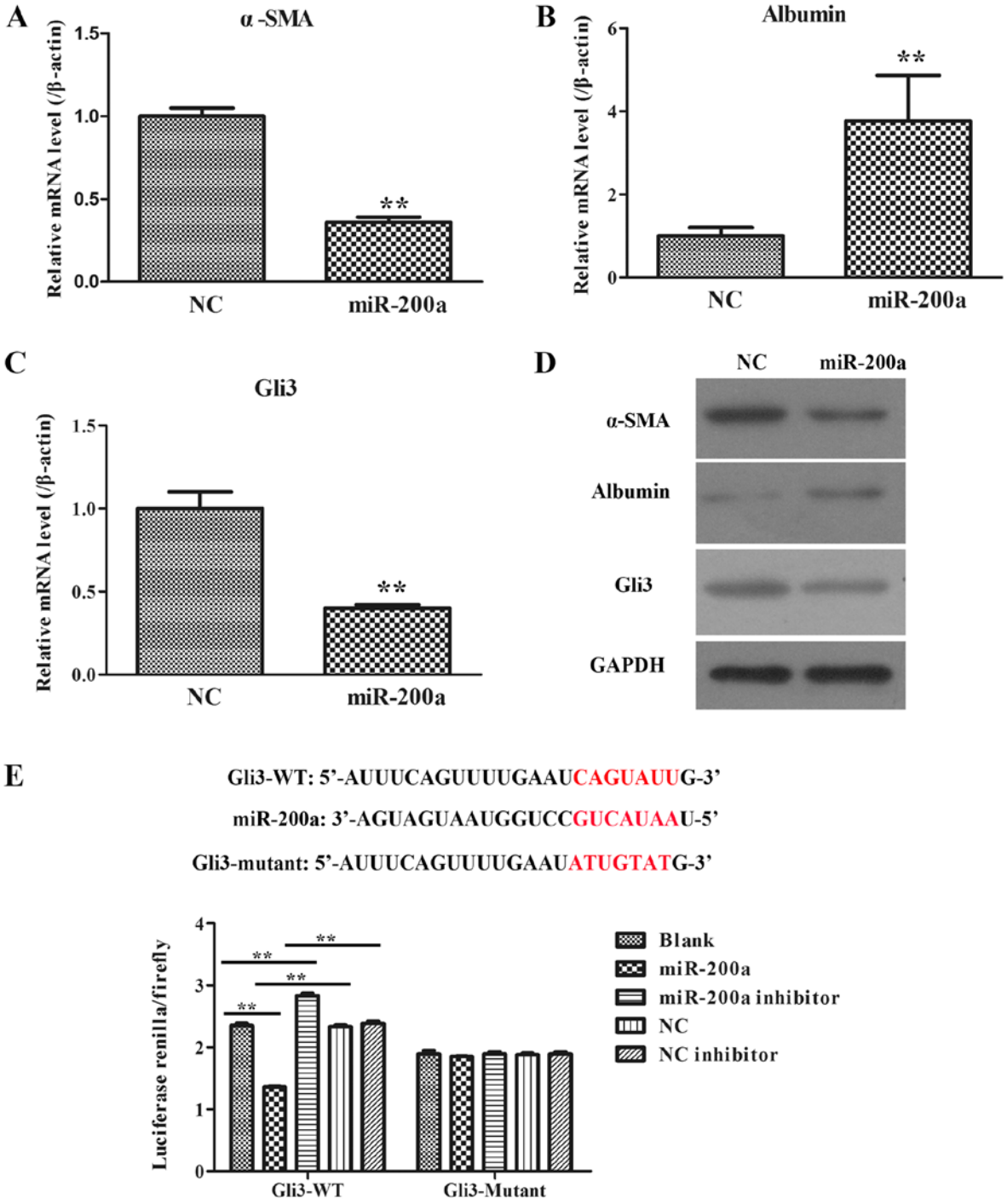

Figure 5. Roles of miR-200A in rat model of liver fibrosis. (A) The mRNA level of α-SMA in liver tissues was analyzed with RT-qPCR. Each value represents the mean ± standard deviation of three experiments. (B) The mRNA level of albumin in liver tissues was examined using RT-qPCR. Each value represents the mean ± standard deviation of three experiments. (C) The mRNA level of Gli3 in liver tissues was examined using RT-qPCR. Each value represents the mean ± standard deviation of three experiments. (D) Protein expression of α-SMA and albumin in liver tissues was analyzed via WB with GAPDH as the internal control. (E) A luciferase reporter assay was performed to determine the direct target binding to the Gli3 mRNA 3' untranslated region by miR-200a. Gli3-Wt-psiCHECK-2 and Gli3-Mut-psiCHECK-2 plasmids were co-transfected with miR-200a mimics or miR-200a inhibitor, respectively, then the luciferase activity was detected. Each value represents the mean ± standard deviation of three experiments. **P<0.01. miR, microRNA; α-SMA, α-smooth muscle actin; RT-qPCR, reverse transcription-quantitative PCR; Gli3, GLI-Kruppel 3; WB, western blot analysis; NC, negative control.

Discussion

Liver fibrosis, which is characterized by the accumulation of ECM, is a common response to many types of liver injury (2). Recently, miRNAs have emerged as key regulators in chronic liver diseases, including hepatic fibrosis (31). For example, miR-145 inhibits HSC activation and proliferation by targeting zinc finger E-box-binding homeobox 2 (ZEB2) through the Wnt/β-catenin pathway (32); miR-222 overexpression may contribute to liver fibrosis in biliary atresia by targeting serine/threonine-protein phosphatase 2A 55 kDa regulatory subunit B α isoform (33). The results of the present study

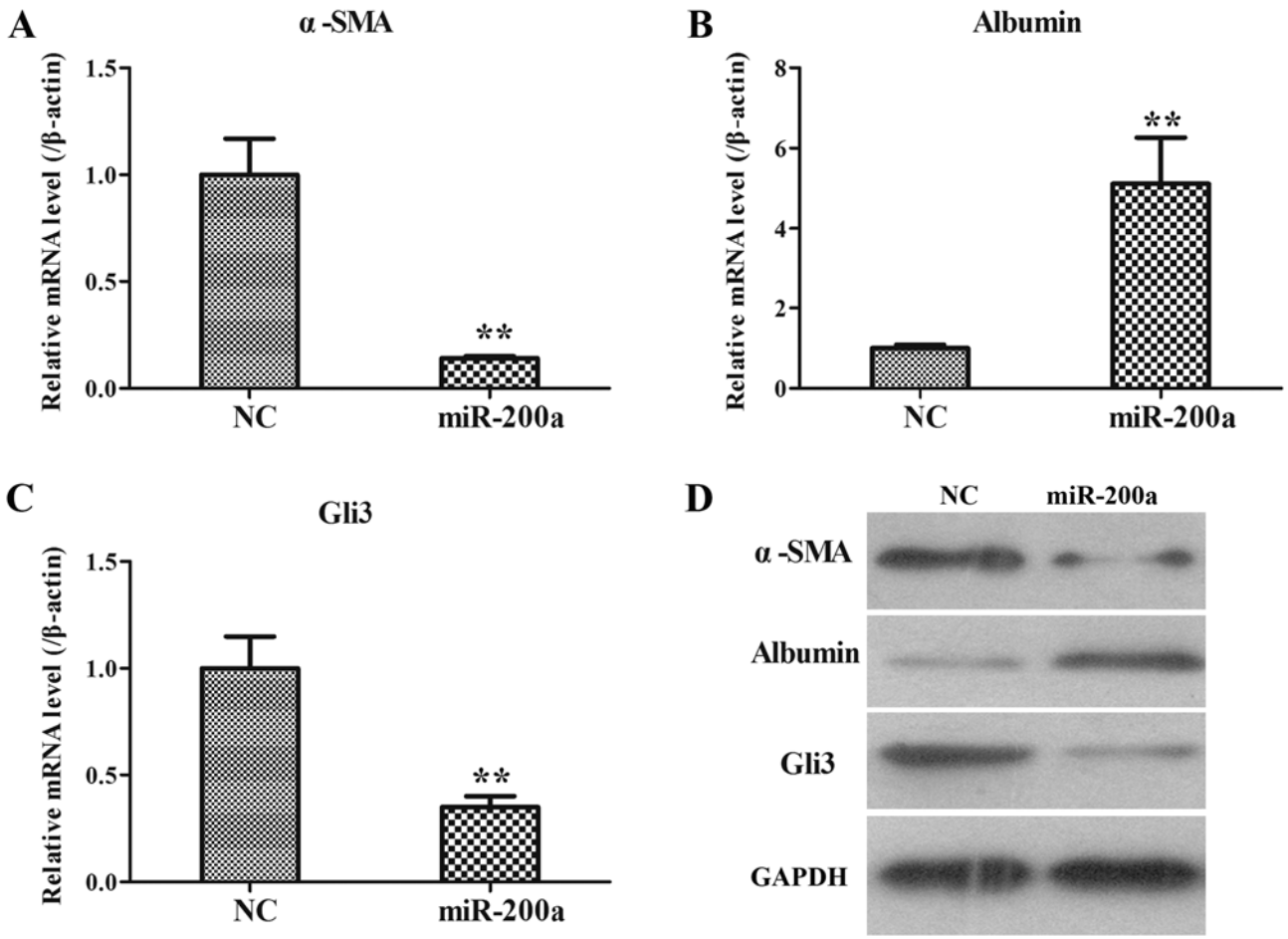

Figure 6. Effect of miR-200a on the expression of key genes associated with rat liver fibrosis. mRNA expression of (A) α-SMA, (B) albumin and (C) Gli3 in LX2 cells and miR-200a-transfected LX2 cells. (D) Protein expression of α-SMA, albumin and Gli3 in LX2 cells and miR-200a transfected LX2 cells. Data are presented as the mean ± SD. **P<0.01 vs. NC group. α-SMA, α-smooth muscle actin; NC, negative control; miR, microRNA.

showed that miR-200a was significantly reduced in serum samples from clinical patients, liver tissues from CCl_4-induced model rats and activated LX2 cells, suggesting that the down-regulation of miR-200a may exert an important role in liver fibrosis.

Fibrogenesis-related indexes, including hydroxyproline content, collagen deposition, α-SMA expression and albumin expression were identified in CCl_4-induced rat models and activated LX2 cells. It was found that the hepatic hydroxyproline content and the Masson's trichrome-positive area in liver tissues from CCl_4-treated rats were apparently increased in comparison with those in control rats. Moreover, the expression levels of α-SMA were also clearly elevated. Therefore, the results indicated that the liver fibrosis of model rats was successfully established. Additionally, it was found that α-SMA and albumin expression at the mRNA and protein levels were markedly upregulated in a co-culture system of LX2 and THP-1 cells. The activation of HSCs is a critical event in the development of liver fibrosis (34). In response to injury, HSCs become activated into proliferative myofibroblasts, migrate into the surrounding parenchymal cells and secrete tissue-damaging ECM (35). It is known that a single miRNA may target >100 mRNAs (36). miR-200a was reported to target ZEB2, thioredoxin-interacting protein/NACHT, LRR and PYD domains-containing protein 3 and insulin-like growth factor 2 to regulate cell growth, hepatic inflammation and placental development (37-39). Recently, the role of Gli3 in liver fibrosis has attracted attention (40). Gli3 is the upstream transcriptional activator of Hh signaling (41). There is emerging evidence that Hh, a master developmental regulator, becomes reactivated during adult wound healing (42). Hh signaling is initiated by the interactions of Hh receptor Patched, Hh ligands (Sonic hedgehog, Indian hedgehog, and Desert hedgehog), and other molecules (such as Gli3) (43). A previous study demonstrated that Gli3 is implicated in the pathogenesis of liver fibrosis via miR-378 regulation (40). In the present study, Gli3 was predicted to be a target of miR-200a. Moreover, the serum Gli3 level in patients with liver fibrosis was negatively related to miR-200a. By using LX2 cells (a common type of HSC), it was also found that forced expression of miR-200a suppressed α-SMA and Gli3 expression and promoted albumin expression. In addition, it was demonstrated that miR-200a could target the 3'-UTR of Gli3, as detected by dual-luciferase reporter assay. Ultimately, at the animal model level, it was further verified that the expression levels of α-SMA and Gli3 were decreased in liver tissues from CCl_4-treated rats injected with miR-200a agomir, whereas the albumin level was enhanced, implying that elevated levels of miR-200a were negatively correlated with Gli3 in activated LX2 cells and rat livers. There is still a limitation in the present study; it only included the serum

samples of the patients. Subsequent experiments may include the collection of liver samples to analyze liver miRNA and Gli3 expression.

Taken together, the results of the present study identified that miR-200a was markedly downregulated during the process of liver fibrosis. The present study also evaluated the target relationship of miR-200a and Gli3. Additionally, restoring miR-200a expression by giving miR-200a mimic in CCl_4-induced liver fibrosis rats and activated LX2 cells could attenuate pro-fibrotic gene expression and enhance anti-fibrotic gene expression. These findings concluded that miR-200a might be a potential target to attenuate liver fibrosis by suppressing Gli3.

Acknowledgements

Not applicable.

Funding

The present study was supported by a Research Fund from the Yunnan Provincial Department of Education (grant no. 2013C239) and a Postdoctoral Supporting Fund from Kunming Human Resources and Social Security Bureau (grant no. 20140298).

Availability of data and materials

The datasets generated and/or analyzed during the present study are available from the corresponding author on reasonable request.

Authors' contributions

LiL and JR made substantial contributions to conception and design. LiL, LaL and GC were involved in the design of the concept, drafting the manuscript and revising it critically for important intellectual content. SZ collected the blood samples of patients and healthy donors, and performed the relevant detection in samples. YW collected and analyzed the data in the animal experiments, and edited the manuscript. All authors read and approved the final manuscript.

Ethics approval and consent to participate

The study protocol was approved by the Ethics Committee of First People's Hospital of Kunming City. The animal experiments were approved by the Ethics Committee of First People's Hospital of Kunming City and complied with the National Institutes of Health Guide for the Care and Use of Laboratory Animals. Prior informed consent was obtained from all patients.

Patient consent for publication

Not applicable.

Competing interests

The authors declare that they have no competing interests.

References

1. Lee UE and Friedman SL: Mechanisms of hepatic fibrogenesis. Best Pract Res Clin Gastroenterol 25: 195-206, 2011.
2. Elpek GÖ: Cellular and molecular mechanisms in the pathogenesis of liver fibrosis: An update. World J Gastroenterol 20: 7260-7276, 2014.
3. Friedman SL: Mechanisms of disease: Mechanisms of hepatic fibrosis and therapeutic implications. Nat Clin Pract Gastroenterol Hepatol 1: 98-105, 2004.
4. Coletta M, Nicolini D, Benedetti Cacciaguerra A, Mazzocato S, Rossi R and Vivarelli M: Bridging patients with hepatocellular cancer waiting for liver transplant: All the patients are the same? Transl Gastroenterol Hepatol 2: 78, 2017.
5. Lim R, Ricardo SD and Sievert W: Cell-based therapies for tissue fibrosis. Front Pharmacol 8: 633, 2017.
6. Treiber T, Treiber N, Plessmann U, Harlander S, Daiß JL, Eichner N, Lehmann G, Schall K, Urlaub H and Meister G: A compendium of RNA-binding proteins that regulate MicroRNA biogenesis. Mol Cell 66: 270-284 e13, 2017.
7. Liu X, Fortin K and Mourelatos Z: MicroRNAs: Biogenesis and molecular functions. Brain Pathol 18: 113-121, 2008.
8. Murakami Y and Kawada N: MicroRNAs in hepatic pathophysiology. Hepatol Res 47: 60-69, 2017.
9. Roderburg C, Urban GW, Bettermann K, Bettermann K, Vucur M, Zimmermann H, Schmidt S, Janssen J, Koppe C, Knolle P, *et al*: Micro-RNA profiling reveals a role for miR-29 in human and murine liver fibrosis. Hepatology 53: 209-218, 2011.
10. Sekiya Y, Ogawa T, Yoshizato K, Ikeda K and Kawada N: Suppression of hepatic stellate cell activation by microRNA-29b. Biochem Biophys Res Commun 412: 74-79, 2011.
11. Ogawa T, Iizuka M, Sekiya Y, Yoshizato K, Ikeda K and Kawada N: Suppression of type I collagen production by microRNA-29b in cultured human stellate cells. Biochem Biophys Res Commun 391: 316-321, 2010.
12. Li J, Ghazwani M, Zhang Y, Lu J, Li J, Fan J, Gandhi CR and Li S: miR-122 regulates collagen production via targeting hepatic stellate cells and suppressing P4HA1 expression. J Hepatol 58: 522-528, 2013.
13. Zhao J, Tang N, Wu K, Dai W, Ye C, Shi J, Zhang J, Ning B, Zeng X and Lin Y: MiR-21 simultaneously regulates ERK1 signaling in HSC activation and hepatocyte EMT in hepatic fibrosis. PLoS On 9: e108005, 2014.
14. He Y, Huang C, Zhang SP, Sun X, Long XR and Li J: The potential of microRNAs in liver fibrosis. Cell Signal 24: 2268-2272, 2012.
15. Yang S, Banerjee S, de Freitas A, Sanders YY, Ding Q, Matalon S, Thannickal VJ, Abraham E and Liu G: Participation of miR-200 in pulmonary fibrosis. Am J Pathol 180: 484-493, 2012.
16. Xu M, Wang G, Zhou H, Cai J, Li P, Zhou M, Lu Y, Jiang X, Huang H, Zhang Y and Gong A: TGF-β1-miR-200a-PTEN induces epithelial-mesenchymal transition and fibrosis of pancreatic stellate cells. Mol Cell Biochem 431: 161-168, 2017.
17. Yang JJ, Tao H, Hu W, Liu LP, Shi KH, Deng ZY and Li J: MicroRNA-200a controls Nrf2 activation by target Keap1 in hepatic stellate cell proliferation and fibrosis. Cell Signal 26: 2381-2389, 2014.
18. Sun X, He Y, Ma TT, Huang C, Zhang L and Li J: Participation of miR-200a in TGF-β1-mediated hepatic stellate cell activation. Mol Cell Biochem 388: 11-23, 2014.
19. Riobo NA and Manning DR: Pathways of signal transduction employed by vertebrate Hedgehogs. Biochem J 403: 369-379, 2007.
20. Bloomsmith MA, Perlman JE, Hutchinson E and Sharpless M: Behavioral management programs to promote laboratory animal welfare: Weichbrod RH, Thompson GAH and Norton JN, (eds). Management of animal care and use programs in research, education, and testing. 2nd edition. Boca Raton (FL): CRC Press/Taylor & Francis, Chapter 5, 2018.
21. Prestigiacomo V, Weston A, Messner S, Lampart F and Suter-Dick L: Pro-fibrotic compounds induce stellate cell activation, ECM-remodelling and Nrf2 activation in a human 3D-multicellular model of liver fibrosis. PLoS One 12: e0179995, 2017.
22. Park EK, Jung HS, Yang HI, Yoo MC, Kim C and Kim KS: Optimized THP-1 differentiation is required for the detection of responses to weak stimuli. Inflamm Res 56: 45-50, 2007.
23. Zhou L, Dong X, Wang L, Shan L, Li T, Xu W, Ding Y, Lai M, Lin X, Dai M, *et al*: Casticin attenuates liver fibrosis and hepatic stellate cell activation by blocking TGF-β/Smad signaling pathway. Oncotarget 8: 56267-56280, 2017.

24. Knight V, Lourensz D, Tchongue J, Correia J, Tipping P and Sievert W: Cytoplasmic domain of tissue factor promotes liver fibrosis in rat. World J Gastroenterol 23: 5692-5699, 2017.
25. Ishak K, Baptista A, Bianchi L, Callea F, De Groote J, Gudat F, Denk H, Desmet V, Korb G, MacSween RN, *et al*: Histological grading and staging of chronic hepatitis. J Hepatol 22: 696-699, 1995.
26. Livak KJ and Schmittgen TD: Analysis of relative gene expression data using real-time quantitative PCR and the 2(-Delta Delta C(T)) method. Methods 25: 402-408, 2001.
27. Rasheed SA, Teo CR, Beillard EJ, Voorhoeve PM and Casey PJ: MicroRNA-182 and microRNA-200a control G-protein subunit α-13 (GNA13) expression and cell invasion synergistically in prostate cancer cells. J Biol Chem 288: 7986-7995, 2013.
28. Kim JY, An HJ, Kim WH, Gwon MG, Gu H, Park YY and Park KK: Anti-fibrotic effects of synthetic oligodeoxynucleotide for TGF-β1 and smad in an animal model of liver cirrhosis. Mol Ther Nucleic Acids 8: 250-263, 2017.
29. King A, Houlihan DD, Kavanagh D, Haldar D, Luu N, Owen A, Suresh S, Than NN, Reynolds G, Penny J, *et al*: Sphingosine-1-phosphate prevents egress of hematopoietic stem cells from liver to reduce fibrosis. Gastroenterology 153: 233-248.e16, 2017.
30. Xu F, Han Y, Zhu D, Tian H, Zhu H, Ren J, Gu D and Duan Y: Construction of a recombinant pIRES2-EGFP-ARTS plasmid and its effect on LX-2 cells. Mol Med Rep 16: 4737-4743, 2017.
31. Jiang XP, Ai WB, Wan LY, Zhang YQ and Wu JF: The roles of microRNA families in hepatic fibrosis. Cell Biosci 7: 34, 2017.
32. Zhou DD, Wang X, Wang Y, Xiang XJ, Liang ZC, Zhou Y, Xu A, Bi CH and Zhang L: MicroRNA-145 inhibits hepatic stellate cell activation and proliferation by targeting ZEB2 through Wnt/β-catenin pathway. Mol Immunol 75: 151-160, 2016.
33. Dong R, Zheng Y, Chen G, Zhao R, Zhou Z and Zheng S: miR-222 overexpression may contribute to liver fibrosis in biliary atresia by targeting PPP2R2A. J Pediatr Gastroenterol Nutr 60: 84-90, 2015.
34. Tsuchida T and Friedman SL: Mechanisms of hepatic stellate cell activation. Nat Rev Gastroenterol Hepatol 14: 397-411, 2017.
35. Zhang CY, Yuan WG, He P, Lei JH and Wang CX: Liver fibrosis and hepatic stellate cells: Etiology, pathological hallmarks and therapeutic targets. World J Gastroenterol 22: 10512-10522, 2016.
36. Friedman RC, Farh KK, Burge CB and Bartel DP: Most mammalian mRNAs are conserved targets of microRNAs. Genome Res 19: 92-105, 2009.
37. Xia H, Ng SS, Jiang S, Cheung WK, Sze J, Bian XW, Kung HF and Lin MC: miR-200a-mediated downregulation of ZEB2 and CTNNB1 differentially inhibits nasopharyngeal carcinoma cell growth, migration and invasion. Biochem Biophys Res Commun 391: 535-541, 2010.
38. Ding XQ, Wu WY, Jiao RQ, Gu TT, Xu Q, Pan Y and Kong LD: Curcumin and allopurinol ameliorate fructose-induced hepatic inflammation in rats via miR-200a-mediated TXNIP/NLRP3 inflammasome. Pharmacol Res 137: 64-75, 2018.
39. Saha S, Choudhury J and Ain R: MicroRNA-141-3p and miR-200a-3p regulate insulin-like growth factor 2 during mouse placental development. Mol Cell Endocrinol 414: 186-193, 2015.
40. Hyun J, Wang S, Kim J, Rao KM, Park SY, Chung I, Ha CS, Kim SW, Yun YH and Jung Y: MicroRNA-378 limits activation of hepatic stellate cells and liver fibrosis by suppressing Gli3 expression. Nat Commun 7: 10993, 2016.
41. Trnski D, Sabol M, Gojević A, Martinić M, Ozretić P, Musani V, Ramić S and Levanat S: GSK3β and Gli3 play a role in activation of Hedgehog-Gli pathway in human colon cancer-Targeting GSK3β downregulates the signaling pathway and reduces cell proliferation. Biochim Biophys Acta 1852: 2574-2584, 2015.
42. Shen X, Peng Y and Li H: The injury-related activation of hedgehog signaling pathway modulates the repair-associated inflammation in liver fibrosis. Front Immunol 8: 1450, 2017.
43. Machado MV and Diehl AM: Hedgehog signalling in liver pathophysiology. J Hepatol 68: 550-562, 2018.